AD-A161 310 THE EFFECTS OF ADDITIVES ON NICKEL ELECRODE DISCHARGE KINETICS..(U) AEROSPACE CORP EL SEGUNDO CA CHEMISTRY AND PHYSICS LAB A H ZIMMERMAN ET AL. 30 SEP 85 1/1

UNCLASSIFIED TR-0084A(5945-01)-1 SD-TR-85-68 F/G 9/1 NL

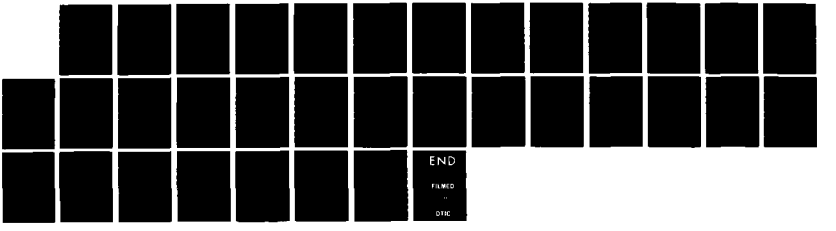

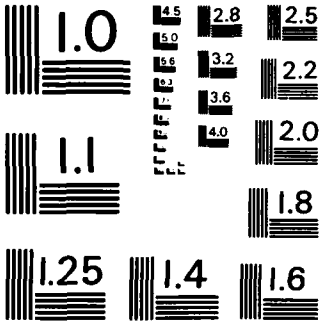

REPORT SD-TR-85-68

(12)

The Effects of Additives on Nickel Electrode Discharge Kinetics

A. H. ZIMMERMAN and P. K. EFFA
Chemistry and Physics Laboratory
Laboratory Operations
The Aerospace Corporation
El Segundo, CA 90245

30 September 1985

APPROVED FOR PUBLIC RELEASE;
DISTRIBUTION UNLIMITED

Prepared for

SPACE DIVISION
AIR FORCE SYSTEMS COMMAND
Los Angeles Air Force Station
P.O. Box 92960, Worldway Postal Center
Los Angeles, CA 90009-2960

This report was submitted by The Aerospace Corporation, El Segundo, CA 90245, under Contract No. F04701-83-C-0084 with the Space Division, P.O. Box 92960, Worldway Postal Center, Los Angeles, CA 90009-2960. It was reviewed and approved for The Aerospace Corporation by S. Feuerstein, Director, Chemistry and Physics Laboratory. Lt Scott W. Levinson, SD/YNS, was the Air Force project officer.

This report has been reviewed by the Public Affairs Office (PAS) and is releasable to the National Technical Information Service (NTIS). At NTIS, it will be available to the general public, including foreign nationals.

This technical report has been reviewed and is approved for publication. Publication of this report does not constitute Air Force approval of the report's findings or conclusions. It is published only for the exchange and stimulation of ideas.

SCOTT W. LEVINSON, Lt, USAF
MOIE Project Officer
SD/YNS

JOSEPH HESS, GM-15
Director, AFSTC West Coast Office
AFSTC/WCO OL-AB

UNCLASSIFIED

SECURITY CLASSIFICATION OF THIS PAGE (When Data Entered)

REPORT DOCUMENTATION PAGE	READ INSTRUCTIONS BEFORE COMPLETING FORM
1. REPORT NUMBER: SD-TR-85-68	2. GOVT ACCESSION NO.: AD-A161310
3. RECIPIENT'S CATALOG NUMBER	
4. TITLE (and Subtitle): THE EFFECTS OF ADDITIVES ON NICKEL ELECTRODE DISCHARGE KINETICS	5. TYPE OF REPORT & PERIOD COVERED
	6. PERFORMING ORG. REPORT NUMBER: TR-0084A(5945-01)-1
7. AUTHOR(s): Albert H. Zimmerman and Peter K. Effa	8. CONTRACT OR GRANT NUMBER(s): F04701-83-C-0084
9. PERFORMING ORGANIZATION NAME AND ADDRESS: The Aerospace Corporation, El Segundo, California 90245	10. PROGRAM ELEMENT, PROJECT, TASK AREA & WORK UNIT NUMBERS
11. CONTROLLING OFFICE NAME AND ADDRESS: Space Division, Los Angeles Air Force Station, Los Angeles, California 90009-2960	12. REPORT DATE: 30 September 1985
	13. NUMBER OF PAGES: 28
14. MONITORING AGENCY NAME & ADDRESS (if different from Controlling Office)	15. SECURITY CLASS. (of this report): Unclassified
	15a. DECLASSIFICATION/DOWNGRADING SCHEDULE

16. DISTRIBUTION STATEMENT (of this Report)

Approved for public release; distribution unlimited.

17. DISTRIBUTION STATEMENT (of the abstract entered in Block 20, if different from Report)

18. SUPPLEMENTARY NOTES

19. KEY WORDS (Continue on reverse side if necessary and identify by block number)

Additives	Lithium
Barium	Manganese
Cadmium	Nickel Electrodes
Cobalt	Resistance
Kinetics	Zinc

20. ABSTRACT (Continue on reverse side if necessary and identify by block number)

The effects of Ba, Cd, Co, Li, Mn, and Zn additives on the impedance of porous nickel electrodes have been measured. The resistance to proton diffusion in the charged electrode is decreased only by Li, Co, and Mn additives. The charge transfer resistance of the nickel electrode can be decreased up to two orders of magnitude by Co and Li additives. The electronic resistance of the discharged active material is reduced

DD FORM 1473 (FACSIMILE)

UNCLASSIFIED

SECURITY CLASSIFICATION OF THIS PAGE (When Data Entered)

19. KEY WORDS (Continued)

20. ABSTRACT (Continued)

significantly by Mn and Co and to a lesser extent by Li. Data are presented indicating that the resistance characteristics correlate with performance during high rate cycling, and that the effects of additives on the physical structure of the active material deposit can be just as important as changes in conductivity.

CONTENTS

FIGURES

I. INTRODUCTION

The effects of additives in the nickel electrode have been widely studied since the work of Edison (1907). The purpose of much of this research has been to change the lattice structure of the nickel oxyhydroxide active material using ionic additives in order to improve particular aspects of electrode performance. As has been pointed out in a review by Weininger (1982), of the large number of additives that have been evaluated, only Co and Li consistently improve electrode performance. Other additives, however, have been reported to improve performance for particular operating conditions or electrode designs. Fritts (1982b) determined that Zn^{+2} improved dimensional stability of sintered electrodes. Li^{+}, Co^{+2}, Zn^{+2}, Cd^{+2}, and Al^{+3} were all found by Weininger (1982) to have some positive effect on capacity and cycle life for flat plate nickel electrodes. Ba^{+2} additives have been used as replacement for Co^{+2} to stabilize performance where Co is scarce. Ag^{+2}, Mn^{+2}, and Fe^{+2} additives have been reported by Jost (1971) to improve charge efficiency by retarding oxygen evolution during recharge, and both Co^{+2} and Mn^{+2} have been found to improve high temperature charge retention by Ritterman et al. (1966).

Several mechanisms may contribute to performance improvements caused by additives. One mechanism is to increase the voltage separation between the nickel oxidation reaction and the oxygen evolution reaction during recharge, an effect which has been observed for Li^{+} additives (Kelson et al., 1973, Takehara et al., 1971) and Mn^{+2} additives (Jost 1971). The changes in recharge voltage relative to oxygen evolution voltage have been found to accompany changes in the extent of incorporation of K^{+} and water from the electrolyte into the crystal lattice (Casey et al., 1965, Weininger 1982, Volynskii and Chernykh 1970). For Co^{+2} additives, there is evidence that performance is improved by altering the relative amounts of β- and γ- NiOOH formed during recharge (Maladin et al., 1978). A second mechanism by which additives may affect performance that may be particularly significant for sintered electrodes is by changing the surface characteristics of the active

material. Weininger (1970) found that for thin film electrodes all additives tested had some positive effect on performance. Sintered electrode studies, which typically involve material with thick film or bulk characteristics, generally have not clearly indicated positive effects from such a wide range of additives.

Studies previously reported in the literature pertaining to how additives affect the nickel electrode have generally focused on how additives affect charge efficiency and the lattice structure of the active materials (Beauchamp and Maurer 1971, Ritterman et al., 1966). Another source of inefficiency in the nickel electrode is the inability to effectively discharge the active material to a low oxidation state, as suggested by the study of Kelson et al. (1973). A detailed study of how additives affect the discharge kinetics of the nickel electrode has not been previously reported. The purpose in this work is to determine the range and types of effects caused by additives on the discharge process in the nickel electrode. The methods employed in this study are to evaluate changes in electrode kinetics caused by various additives by impedance measurements and to measure the cycling performance of these nickel electrodes.

II. EXPERIMENTS

Electrodes were made by cathodic polarization of 1 cm^2 pieces of nickel sinter in a solution consisting of 60% 2M nickel nitrate and 40% ethanol by volume. During polarization, the solution was held at a reflux temperature of about 80°C, and the polarization current was 35 mA/cm^2 unless indicated to be otherwise. Polarization time was typically 3 hr. The nickel sinter used was 0.076 cm thick and contained 82% void volume. This process provided electrodes with a loading of about 1.60 g/cc void and a typical capacity of 20 to 30 mAh. Additives were introduced during the polarization process by replacing 5% of the nickel nitrate with the same molar amount of the additive metal nitrate, with the exception of Li additive, which was added directly to the electrolyte as LiOH.

The electrolyte was 31% potassium hydroxide by weight, which was made by diluting a 45% reagent solution of KOH (J. T. Baker). Lithium additives were incorporated into the electrodes by replacing 3% of the KOH with reagent grade LiOH giving an electrolyte composed of 28% KOH and 3% LiOH. No attempt was made to vary the amount of LiOH in the electrolyte.

The electrodes were cycled in a closed polystyrene cell. A continuous slow nitrogen purge minimized contamination by atmospheric CO_2. All electrodes were studied in a flooded state. The reference electrode was an Hg/HgO electrode enclosed in a small polyethylene tube that was immersed in the electrolyte adjacent to one corner of the nickel test electrode. Electrolytic contact from the reference electrode to the cell electrolyte was made by a nylon wick that passed through a pinhole in the polyethylene tube. All impedance and resistance data have been compensated for electrolyte resistance between the reference and working electrodes. Compensation was done by a current interruption method and was typically 0.3 to 1.0 Ω. The counter electrode was a 4 cm^2 piece of nickel sheet. Cell temperature was 22 ± 2°C.

Charge/discharge cycling was under the control of a computer, which in addition to controlling charge and discharge at constant current or voltage, also automatically measured electrode impedance as a function of frequency and

monitored electrode voltage and current. The impedance was measured during constant current discharge by applying a stepwise current perturbation of sufficient magnitude to cause about a 5 mV change in the electrode voltage. The voltage time response was monitored and stored by the computer with a 1 msec resolution and was subsequently used to determine the impedance. After the experiment was completed, Laplace transformation of the voltage and current allowed the impedance to be determined as a function of frequency from DC up to 500 Hz (Pilla 1970).

After fabrication, rinsing, and drying, each electrode was cycled three times to stabilize and evaluate the initial performance. Each cycle involved charge for 10 hr at 6 mA/cm^2 followed by sequential discharges to -0.5 V vs. Hg/HgO at 6, 1.5, and 0.3 mA/cm^2, respectively. The capacity of each electrode, C, was defined by the total capacity discharged on the third cycle. The electrode was then cycled twice using a C/5 charge for 10 hr followed by C/5 discharge to 1.1 V and a C/100 discharge to -0.5 V. During the second discharge cycle the computer was programmed to periodically measure the impedance during the C/5 and the C/100 discharge.

Long-term cycling of the test electrodes was performed for 1000 cycles, and each cycle consisted of recharge at 150 mA/cm^2 followed by discharge at 150 mA/cm^2 to -0.5 V vs. Hg/HgO. The recharge time was such that the charge returned on each cycle was equal to the initial electrode capacity discharged at a rate of 15 mA/cm^2 to -0.5 V (after recharge 15 mA/cm^2 rate).

III. RESULTS AND DISCUSSION

A. DIFFUSION IMPEDANCE

The impedance characteristics of nickel electrodes have been the subject of several recent studies (Madou and McKubre 1983, Zimmerman and Effa 1984) that indicate how the electrode impedance changes with voltage and state of charge. These studies and other previous investigations (Takehara et al., 1971, Zimmerman and Janecki 1982) have shown that at normal operating voltages and states of charge, nickel electrode discharge is controlled by a diffusion process, which has been identified by MacArthur (1970a,b) as solid-state proton diffusion in the nickel oxyhydroxide lattice. The impedance caused by the proton diffusion process is indicated during discharge at the C/5 rate in Fig. 1. The diffusion resistance R_D defined in Fig. 1 provides a measure of the extent of electrode polarization caused by the diffusion process and serves as a useful parameter to compare the effects of additives to the diffusion process. Fig. 2 indicates how R_D changes with electrode state of charge during a C/5 discharge for nickel electrodes having various additives.

The data in Fig. 2 indicate three distinct regions: a high state of charge region where R_D increases rapidly with decreasing state of charge, an intermediate region where R_D is relatively constant, and a low state of charge region where R_D again increases with continued discharge. The very low R_D at high states of charge may arise from rapid proton diffusion to highly active charge transfer sites generated during recharge at the active material/electrolyte interface. R_D should rise sharply as these reactive sites are depleted, and then level off as the bulk active material discharges. As the state of charge is reduced, the charged sites in the active material lattice become depleted, and since such sites are required for lattice proton migration (MacArthur 1970a,b), the measured R_D increases as low states of charge are approached. The effects of the additives indicated in Fig. 2 fall into three general categories. Cadmium appears to have little effect on R_D, whereas Co and Li decrease R_D, and Zn and Ba appear to increase R_D. The effect of the additives seems to be primarily in the plateau resistance and

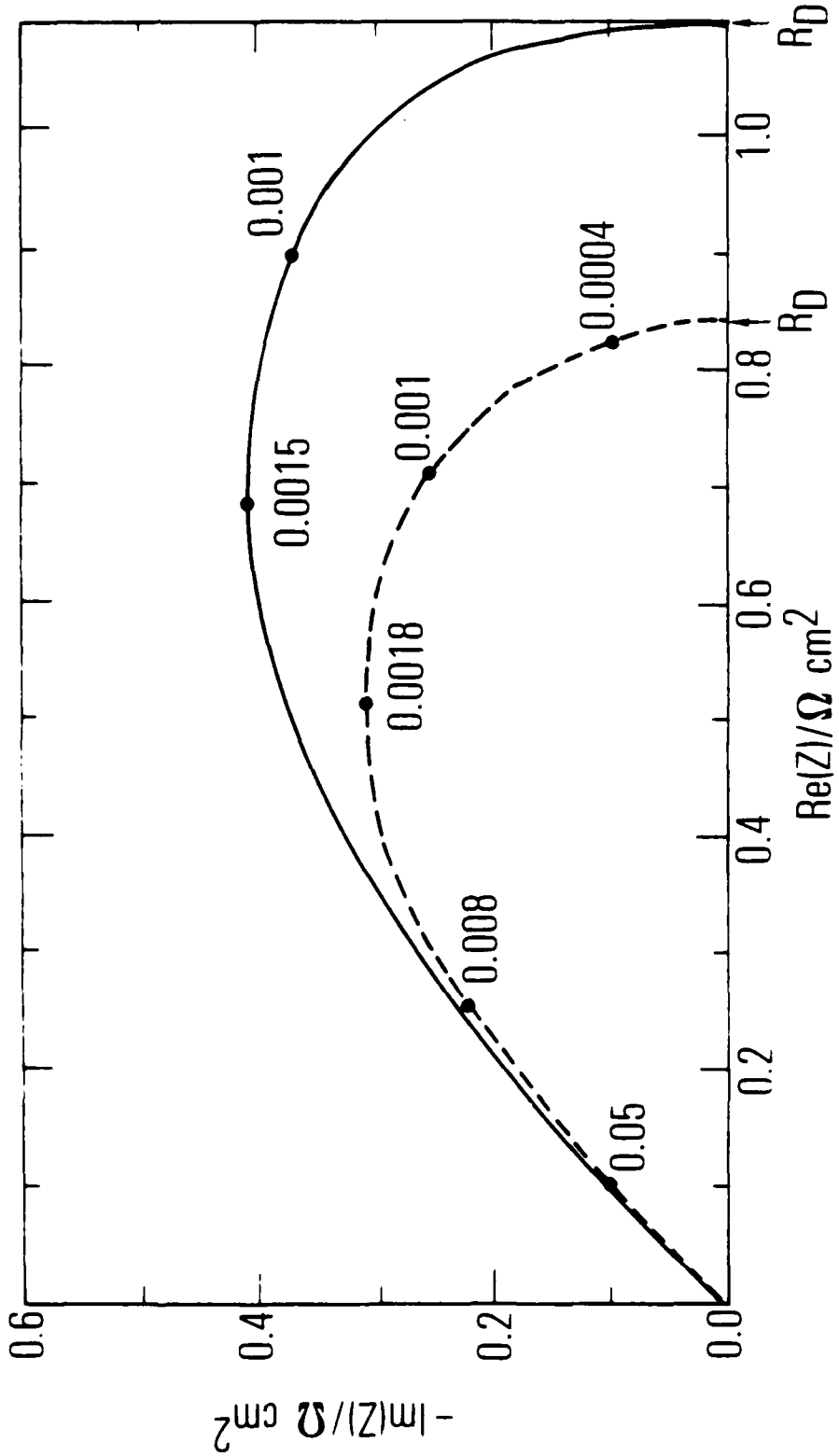

Fig. 1. Nickel Electrode Impedance During a C/5 Discharge Without Additives (——) and With 5% Co Additive (---). The numbers indicate frequency in Hz. The diffusion resistance R_D is marked on the x-axis for each electrode.

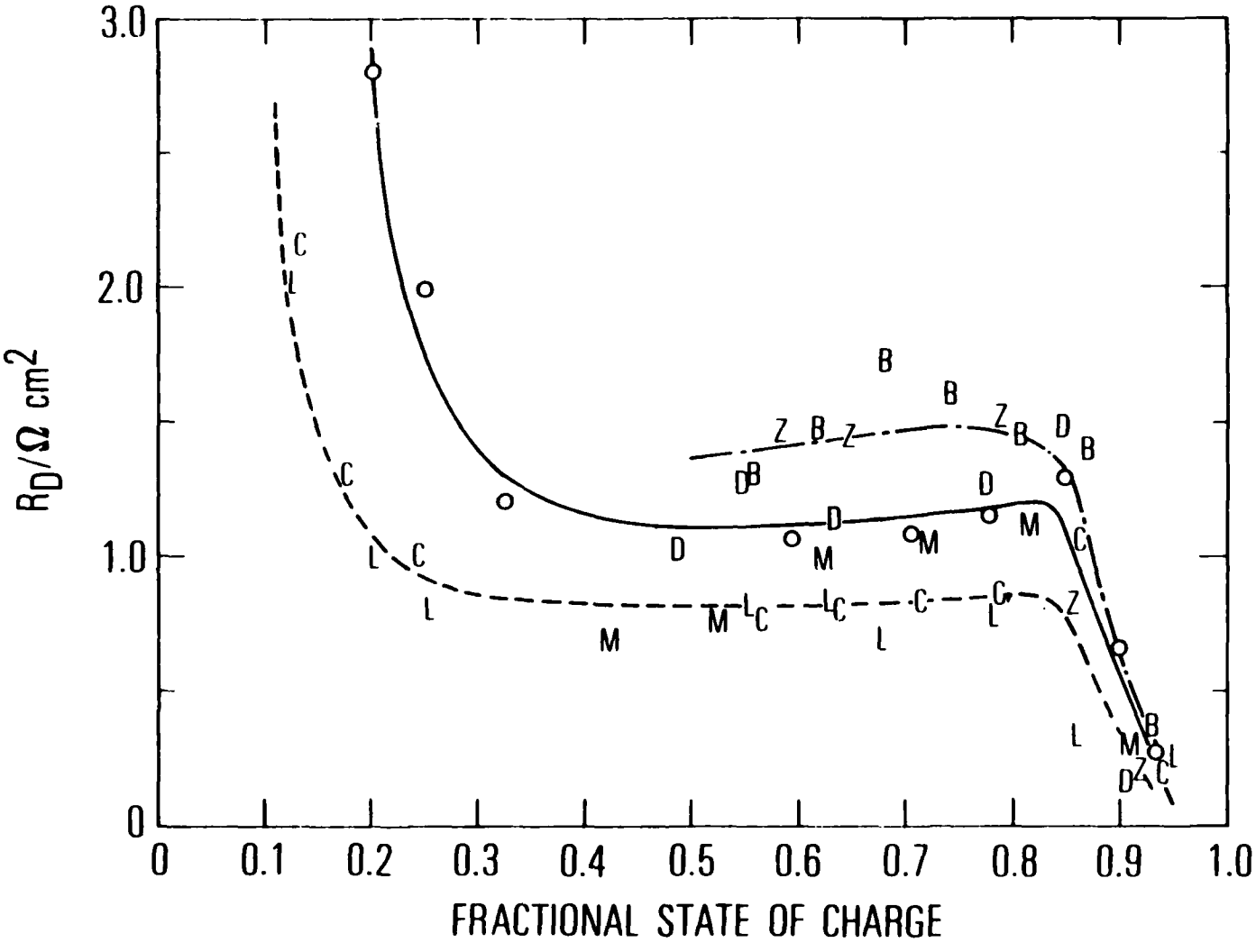

Fig. 2. Effect of Additives on the Diffusion Resistance of Nickel Electrodes at a C/5 Discharge Rate. Zero on the x-axis corresponds essentially to a divalent oxidation state and 1.0 to the maximum oxidation state reached by each electrode. No additives are indicated by circles; L = lithium, C = cobalt, M = manganese, D = cadmium, B = barium, and Z = zinc. All additives are present at a concentration of 5%, except Li, which is 3% in the electrolyte.

the rise in resistance at low states of charge. Manganese additives give somewhat different behavior, causing little effect above about 0.7 state of charge, but below 0.7, the resistance decreases to values similar to Co and Li. R_D in the low state of charge region measured at the C/100 rate is plotted in Fig. 3 for nickel electrodes with no additives, 5% Co, and 3% Li additives. Fig. 3 indicates that R_D adopts a logarithmic dependence on state of charge, a dependence that is reasonable for asymptotic depletion of charge carriers in the active material as it approaches the discharged state. Again the presence of Co or Li causes a significant decrease in R_D without affecting its overall variation with state of charge.

The relationship between state of charge as indicated in Fig. 2 and residual capacity in Fig. 3 is provided by the capacities in Table 1. Residual capacity is the amount of the total that cannot be discharged at the C/5 rate above 1.1 V, and state of charge is the fraction of the total that remains. Table 1 generally indicates that total capacity is improved somewhat by all additives except Ca, which has little effect. The additives Co and Mn show the largest improvement, about 20% of the total.

Table 1. Test Electrode Capacities with Various Additives at C/100 Discharge Rate

Various Additives	Capacity, mAh
No Additives	29.01
3% Lithium	33.90
5% Cobalt	36.22
3% Lithium + 5% Cobalt	32.87
5% Manganese	35.96
5% Barium	34.82
5% Zinc	31.80
5% Cadmium	28.14

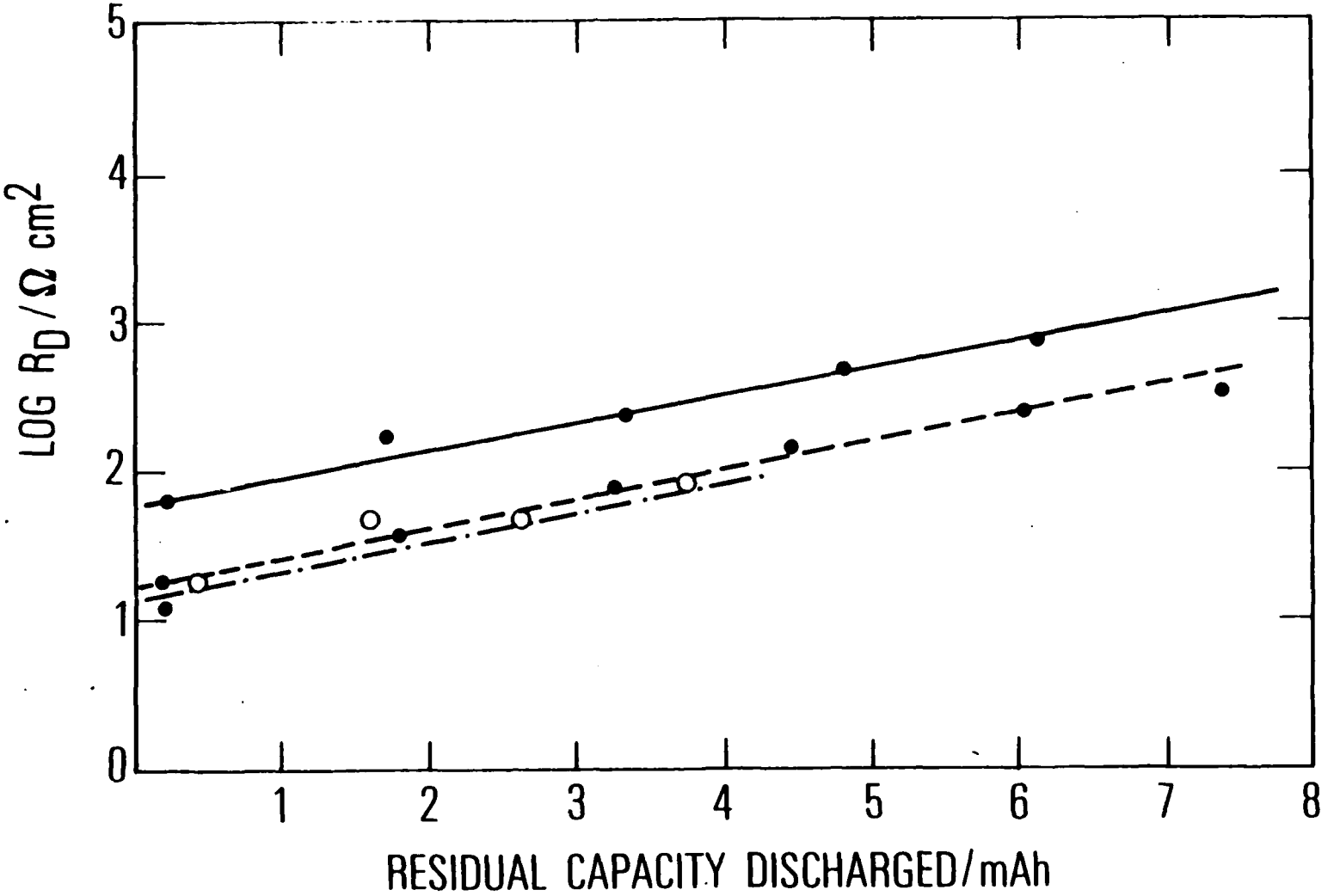

Fig. 3. Effect of Li and Co Additives on the Diffusion Resistance in Nickel Electrodes During Discharge of Residual Capacity at a C/100 Rate. Without additives (——), 3% Li in electrolyte (-•-), 5% Co additive (---).

Several explanations may be proposed to account for the effects of additives on the diffusion resistance, as indicated in Figs. 2 and 3. One explanation is that the incorporation of the additives into the active material lattice structure alters the lattice structure such that protons may move more or less freely. For Li and Co, such incorporation into the lattice structures has been proposed (Weininger 1982) and is supported by the fact that these were the only additives that significantly reduced the open circuit potential of the electrode. The results obtained here suggest that Co, Li, and possibly Mn additives provide defects in the active material lattice that can substantially decrease the resistance of this lattice to ionic conduction. The other additives did not appear to show a decrease in R_D. This may be the result of ineffective incorporation into the active material lattice (e.g., the additives segregate and do not remain dispersed through the lattice), or these additives may provide lattice sites having either little influence or a trapping influence on charge carriers, which could actually increase resistance. Another possibility that must be considered in explaining the effects of additives is the influence of active material morphology on the resistance. Additives such as Ba, Zn, and Mn were noted to yield deposits of active material that tended to appear less compact than for the other additives, and did not appear to penetrate the sinter as effectively. A more agglomerated active material structure, if present at the microscopic pore level, would be expected to have higher ionic resistance characteristics caused by greater diffusion lengths. It is possible that Ba and Zn with additives have a diffusion resistance greater than without additives because of such variation in the physical structure of the active material, and that Mn also suffers in this regard relative to electrodes containing Co or Li.

B. CHARGE TRANSFER IMPEDANCE

As the nickel electrode active material is discharged towards the divalent state, the impedance begins to become controlled by an electrochemical process that is activation controlled, in addition to the diffusion controlled process observed at higher oxidation states. The activation controlled behavior has been studied by Madou and McKubre (1983) and Zimmerman

and Effa (1984); it has also been identified with charge transfer processes in the nickel electrode. At voltages above 0.2 vs. Hg/Hgo, the charge transfer resistance has been proposed (Zimmerman and Effa 1984) to result from electrochemical charge transfer associated with reduction of the charged active material, whereas below 0 V vs. Hg/HgO the charge transfer resistance appeared to be more consistent with charge transfer across an interfacial barrier layer. The barrier layer is presumed to form at the metal/hydroxide interface as a result of preferred discharge and depletion of charge carriers at this interface. The form of the impedance in each of these voltage regions is indicated in Fig. 4. Fig. 4 defines the charge transfer resistance R_c and the diffusion resistance R_D at the higher voltages, as well as the charge transfer resistance R_c' at the lower voltages. The two types of charge transfer resistances, R_c and R_c', are differentiated by the dependence on electrode voltage indicated in Fig. 5.

The effect of additives on R_c and R_c' is to either reduce or to have little effect on the resistance at a given voltage. The range of resistance decreases that were observed are indicated in Fig. 5, and the resistance with Co and Co/Li additives is compared with the resistance without additives. Also indicated in Fig. 5 is the shift in open circuit potential caused by these additives. The data in Fig. 5 may be plotted as a function of residual capacity (capacity Q unavailable at C/5 rate), as shown in Fig. 6. The resistance peak in the plot of Fig. 6 occurs at the point where the characteristic voltage dependence of the resistance changes in the vicinity of 0.1 V, and therefore the resistance prior to the peak reflects R_c and after the peak R_c'. From Fig. 6 it can be concluded that R_c is significantly reduced by both Li and Co additives, with the effects of these two additives together being roughly equal to the sum of their individual effects. Also, the rate of increase in R_c with extent of discharge is much less for electrodes with Co additives than for electrodes without an additive or only Li additives. This suggests that the Co oxyhydroxide species in the lattice may reduce resistance by actually providing additional charge carriers that can maintain ionic conductivity. None of the other additives, the remainder of which are presented in Fig. 7, provide this kind of modification to R_c.

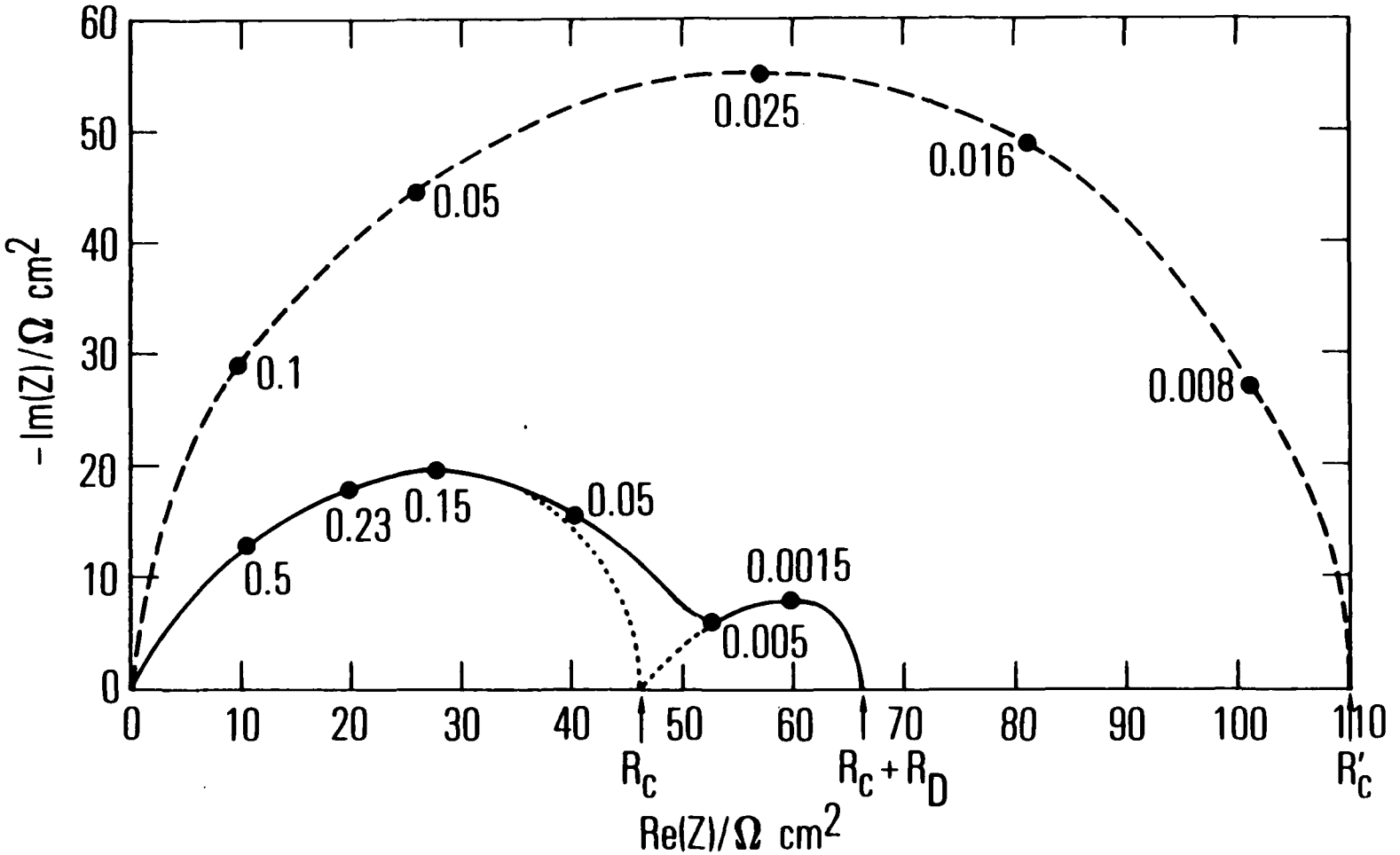

Fig. 4. Impedance Plot During a C/100 Discharge of a Nickel Electrode Containing 5% Co at 0.29 (——) and 0.0 V (---) vs. Hg/HgO. The impedance at 0.0 V has been divided by 5, and the numbers indicate frequency in Hz on each curve. R_D indicates the diffusion resistance, R_c the charge transfer resistance, and R_c' the barrier layer resistance.

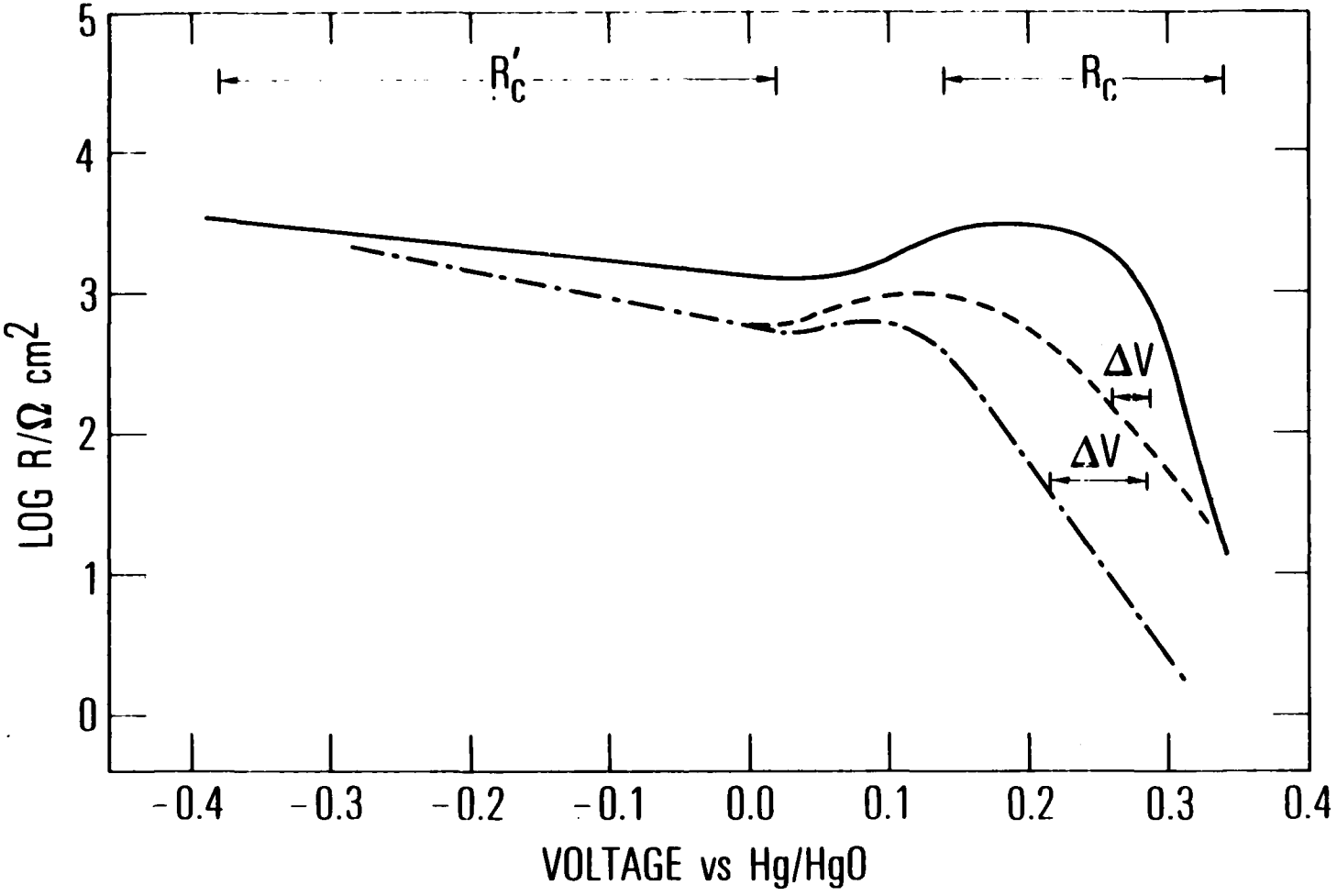

Fig. 5. Resistance as a Function of Voltage During a C/100 Discharge for Nickel Electrodes Without Additives (——), 5% Co Additive (---), and 5% Co + 3% Li Additive (-·-). R_c and R_c' indicate the regions of charge transfer and barrier layer conduction control of the discharge process. The ΔV ranges marked on the curves indicate the shift in open circuit voltage for the electrodes with additives relative to that without additives at a state of charge of about 0.25.

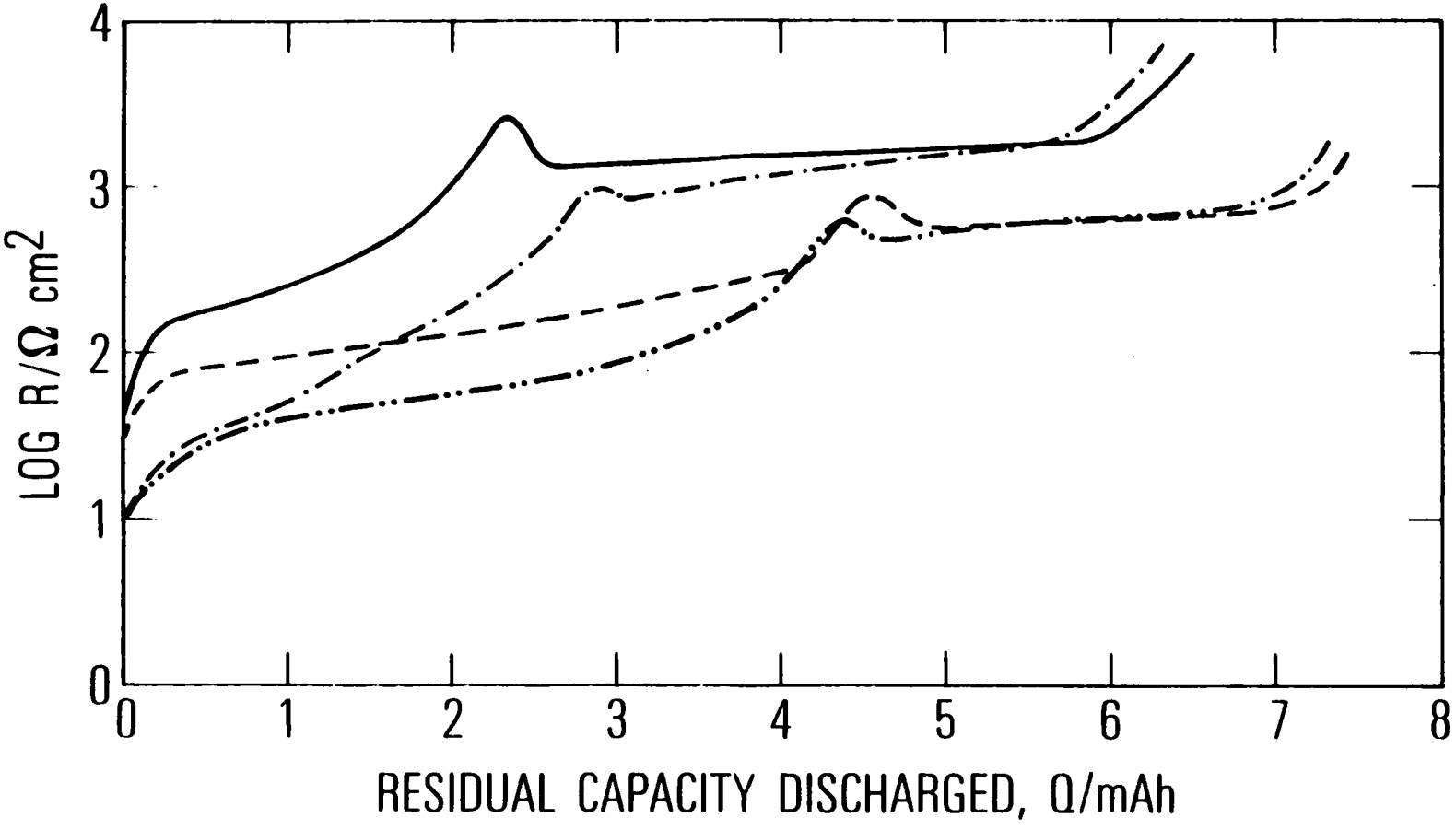

Fig. 6. Resistance as a Function of Residual Capacity Discharged at the C/100 Rate for Nickel Electrodes Without Additives (——), 3% Li (-•-), 5% Co (---), and 3% Li + 5% Co (-••-).

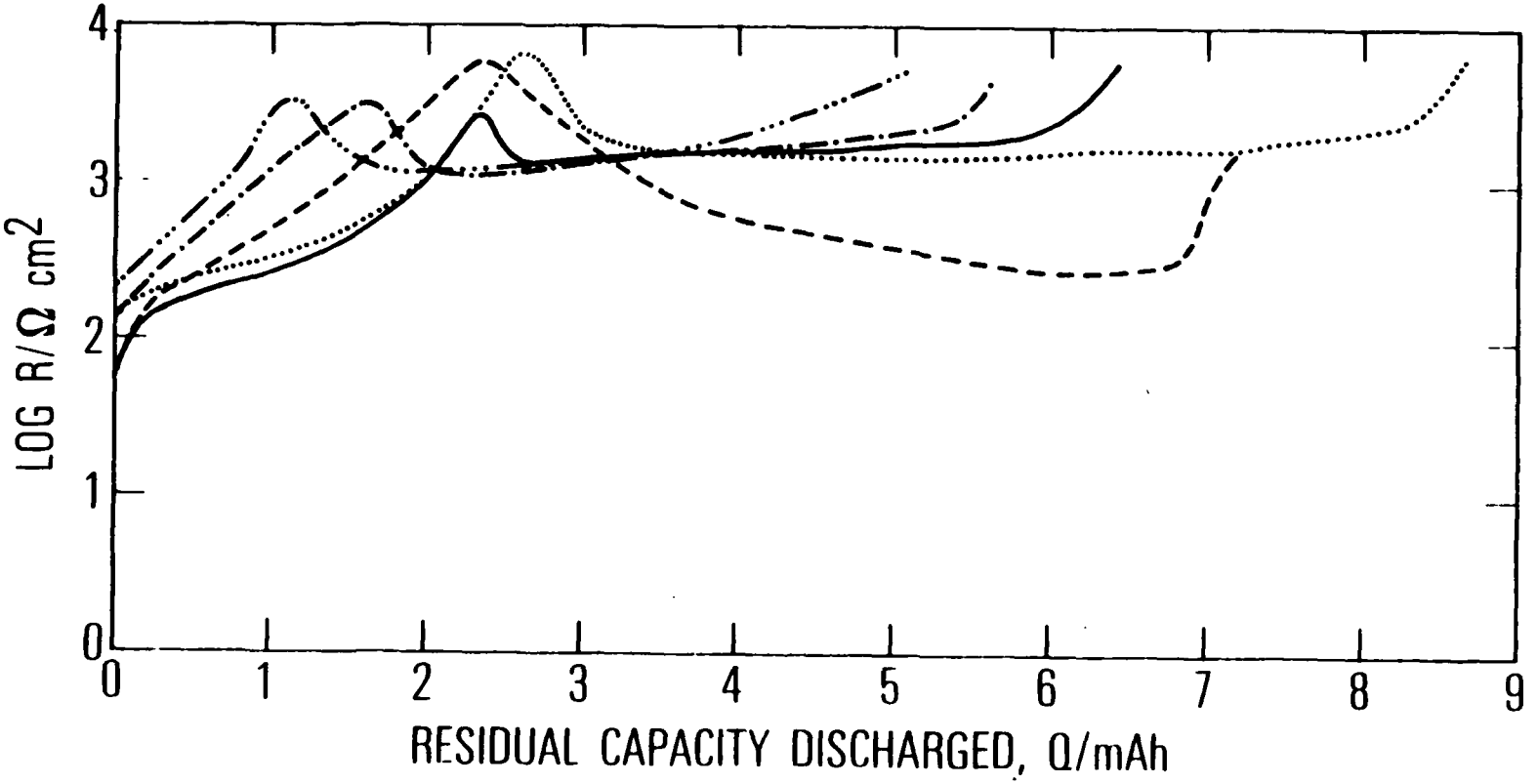

Fig. 7. Resistance as a Function of Residual Capacity Discharged at the C/100 Rate for Nickel Electrodes Without Additives (——), 5% Mn (– – –), 5% Zn (–•–), 5% Ba (••••), and 5% Cd (–•••).

The barrier layer resistance R_c', observed below 0 V, was significantly affected only by Li, Co, and Mn. For the Co additive, R_c' was much lower than without any additive, and exhibited very little dependence on extent of discharge. The only additives that did cause R_c' to vary with extent of discharge were Li and Mn. For Li, additive R_c' is reduced initially, but then rises with continued discharge to approximately the same value as when additives are not present. Very unusual behavior was exhibited by Mn additives. As shown in Fig. 7, R_c' for the electrode with Mn additive decreased to a very low value (even lower than with Co) near the point where its capacity was totally discharged. However, with Mn present the resistance does not adopt the characteristic logarithmic dependence on voltage in the low voltage region until the resistance has dropped to low values near the end of discharge. This is because the electrode with Mn has an extremely wide range of capacity over which the transition occurred from high voltage, charge-transfer reaction limited behavior to lower voltage, barrier layer-dominated behavior. The behavior of the electrode with the Mn additive may be caused by the formation of an extremely nonuniform barrier layer, a situation for which the barrier layer of discharged material forms over an extremely wide range of capacity. In this context the width of the resistance peaks in Figs. 6 and 7 reflect the uniformity with which the active material is discharged in the region of the metal/hydroxide interface.

Lithium additives were incorporated into the nickel electrodes directly from Li^+ ions in the electrolyte. It has been suggested that the process is reversible and that the extent of incorporation depends on the amount of γ-NiOOH phase or other charged phases that incorporate the alkali ions (Weininger 1982) during recharge. If this is correct the effects of Li on nickel electrode resistance should be eliminated by rinsing the Li^+ species from the totally discharged electrode. The effect of applying lithiated electrolyte, and then the effect of replacing the lithiated electrolyte with pure KOH is indicated in Fig. 8. R_c shows a significant decrease with Li present as expected, but returned to its original level when the lithiated electrolyte was removed. However, the slight decrease in R_c' that results from the Li additive is not eliminated, suggesting that small amounts of Li^+

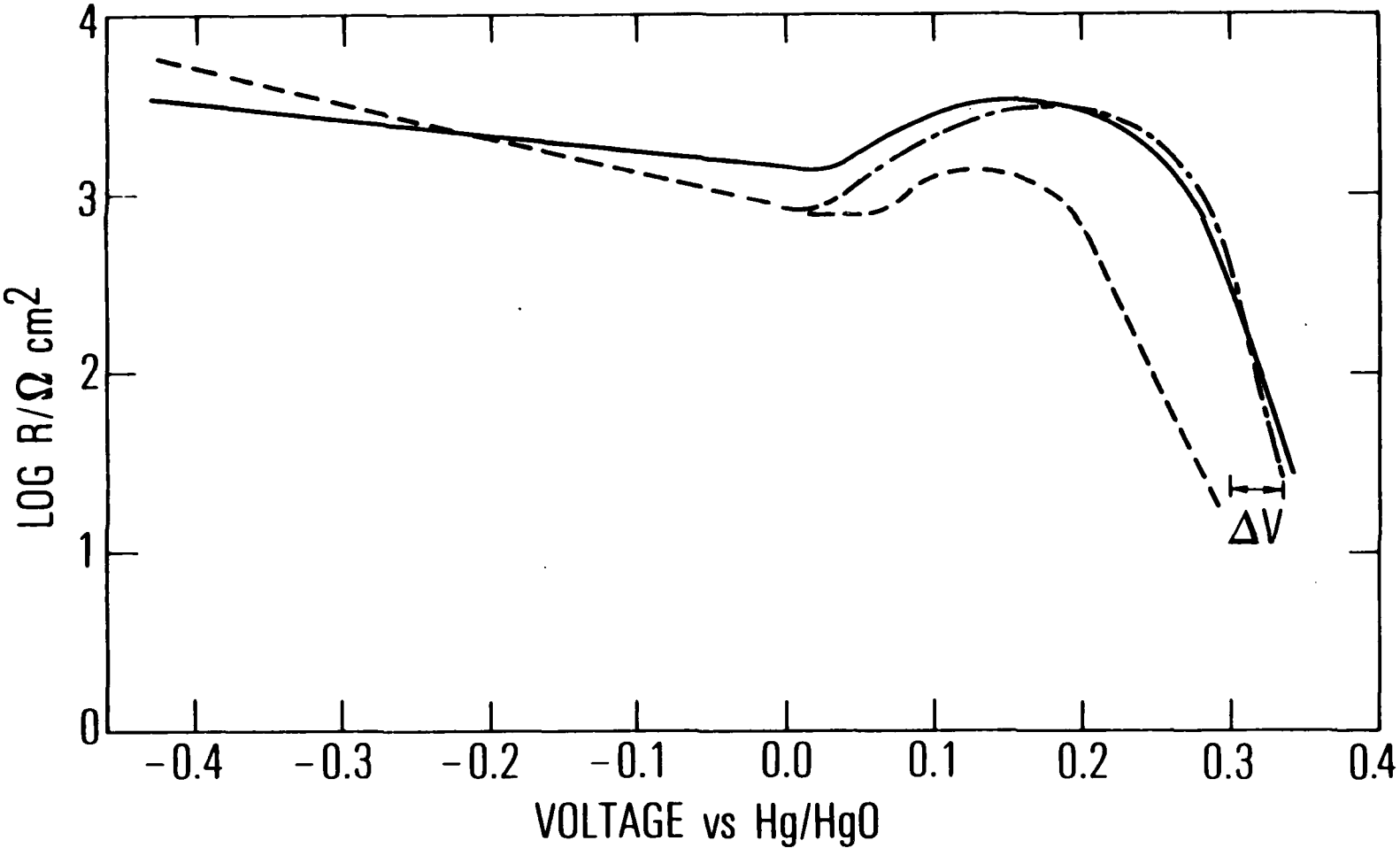

Fig. 8. Resistance as a Function of Voltage During a C/100 Discharge of Residual Capacity in a Nickel Electrode: (1) Without Additives (——), (2) After Addition of 3% Li to the Electrolyte (---), and (3) After Removal of Lithiated Electrolyte (→→). The indicated ΔV is the shift in open circuit potential with Li at a fractional state of charge of about 0.2.

species retained in the discharged active material are sufficient to affect its electronic conductivity.

C. CHARGE/DISCHARGE PERFORMANCE

Measurements by Fritts (1981, 1982a) have indicated that internal strain in sintered electrodes can contribute to capacity degradation over long-term cycling, and that such strain levels are highly dependent on additives. Several electrodes were cycled extensively in this study using relatively high charge and discharge rates to determine whether the early life impedance characteristics that have been measured for various additives correlate with cycle life performance.

The performance of nickel electrodes without additives is indicated in Fig. 9 for charge/discharge rates of 150 mA/cm^2. The two electrodes indicated in Fig. 9 were prepared at different deposition temperatures, 80°C being the normal reflux temperature used in electrode preparation. The higher temperature is expected to impact performance largely by maintaining a more uniform concentration of reagents in the pore structure during deposition, and thereby giving a more uniform deposit of active material. The data in Fig. 9 show a trend that is characteristic of this kind of cycling test. The capacity rises for a number of cycles, then begins to fall rapidly before leveling off at a capacity of about 30% of the theoretical capacity. If it is assumed in Fig. 9 that the major difference between the two electrodes is that the electrode produced at 20°C has the less uniform deposit of active material, then the region of rapidly falling capacity can be identified with physically nonuniform active material in the pore structure. Although the nature of the suggested nonuniform structure cannot be defined from the electrical performance, scanning electron microscopy of cross-sectioned nickel electrodes indicates that it consists of an active material deposit that is heavier near the opening of the pores in the sinter.

The major change in the impedance of the nickel electrodes as a result of the cycling in Fig. 9 is that the upturn in R_D at low states of charge indicated in Fig. 2, and the peak in resistance indicated in Figs. 5 through 7, occurs at states of charge that increase as the electrode capacity decreases (residual capacity increases). The dependence of resistance on electrode

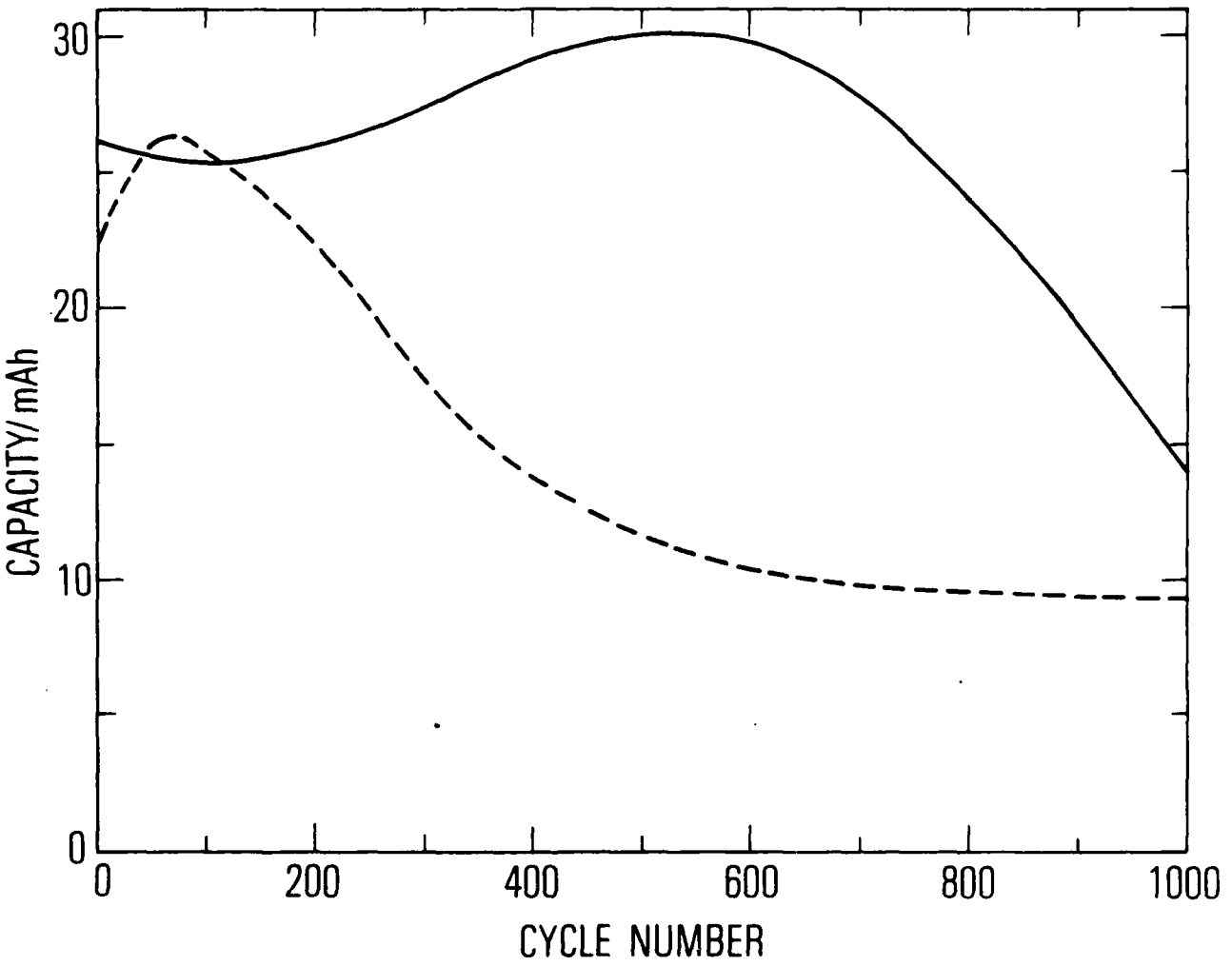

Fig. 9. Capacity as a Function of Cycle Number for Nickel Electrodes Fabricated Using a Deposition Temperature of 80°C (——) and 20°C (---), and Having Initial Theoretical Capacities (One Electron Change) of 27.7 and 29.5 mAh, Respectively. Charge and discharge rates are 150 mA/cm^2. These electrodes contain no additives.

voltage is not changed dramatically by the cycling. The resistance peak limits high rate capacity and has been previously identified (Zimmerman and Effa 1984) with the formation of an isolating layer of discharged material at the boundary between the sinter and the active material. It is therefore reasonable that changes in active material morphology, which can cause large changes in the interfacial area and current density, should be an important factor in determining the state of charge at which the resistance peak occurs. In all cases the loss of capacity during cycling did not correspond to either shedding of active material, or to any coulombic inefficiency in electrode recharge (although the recharge voltages did rise in a way that would have caused recharge efficiency to decrease if constant voltage recharge procedures were employed). All the original capacity could eventually be discharged from the degraded electrodes at very low rates, as expected where capacity is limited by isolation of active material.

Electrodes containing additives such as Co or Li are likely to be much less susceptible to performance degradation caused by nonuniformities in active material deposition because their resistance, R_c, is reduced by nearly an order of magnitude over electrodes without additives. The performance of electrodes with the Co additive produced at several current densities is indicated in Fig. 10. The electrodes produced at a deposition rate of 35 mA/cm^2 or less showed no degradation of the kind seen in Fig. 9 when additives were not present. However, even with the Co additive, doubling the current density during deposition to 70 mA/cm^2 decreases the apparent electrode uniformity to the point where significant degradation of capacity is observed with cycling.

Electrodes that contain additives other than Li or Co do not have a reduced interfacial resistance, R_c, at the boundary between the metal and the active material (Fig. 7), and are therefore not likely to provide improvement in discharge utilization over electrodes without additives. The performance of electrodes containing Zn or Mn additives is indicated in Fig. 11 and clearly shows degraded cycle life capability for these electrodes. The degradation was particularly severe in the case of the Zn additive, which was taken off the test after 700 cycles because the end of charge voltage was approaching 1.0 V vs. Hg/HgO (0.65 V was typical for properly functioning electrodes at 150 mA/cm^2).

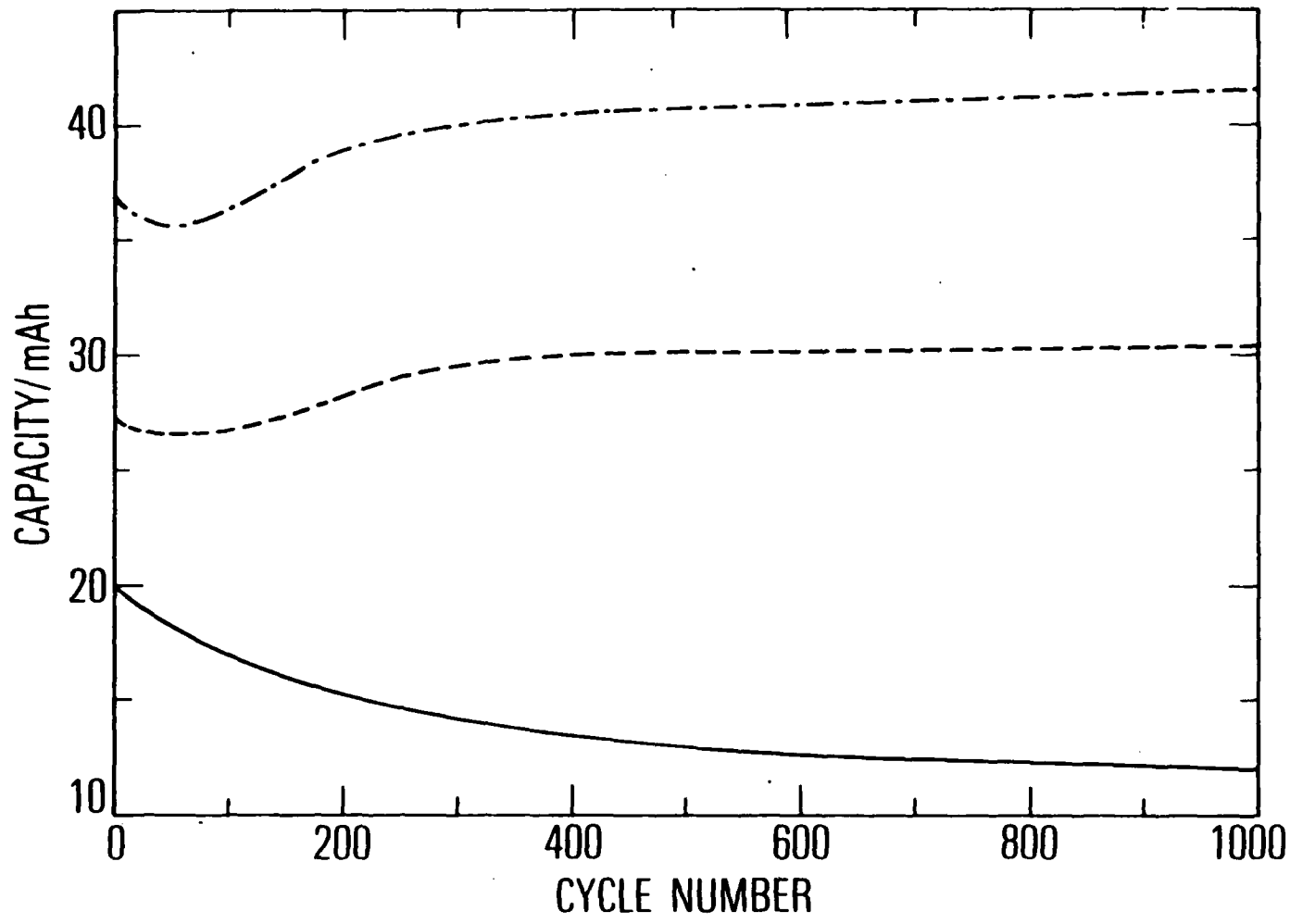

Fig. 10. Capacity as a Function of Cycle Number for Nickel Electrodes Containing 5% Co, and Fabricated Using Deposition Rates of 70 mA/cm^2 for 1.5 hr (——), 35 mA/cm^2 for 3 hr (---), and 20 mA/cm^2 for 6 hr (-·-). The deposition temperature was 80°C. The initial theoretical capacities based on a one electron change are 26.7, 32.2, and 37.4 mAh, respectively. Charge and discharge rates are 150 mA/cm^2.

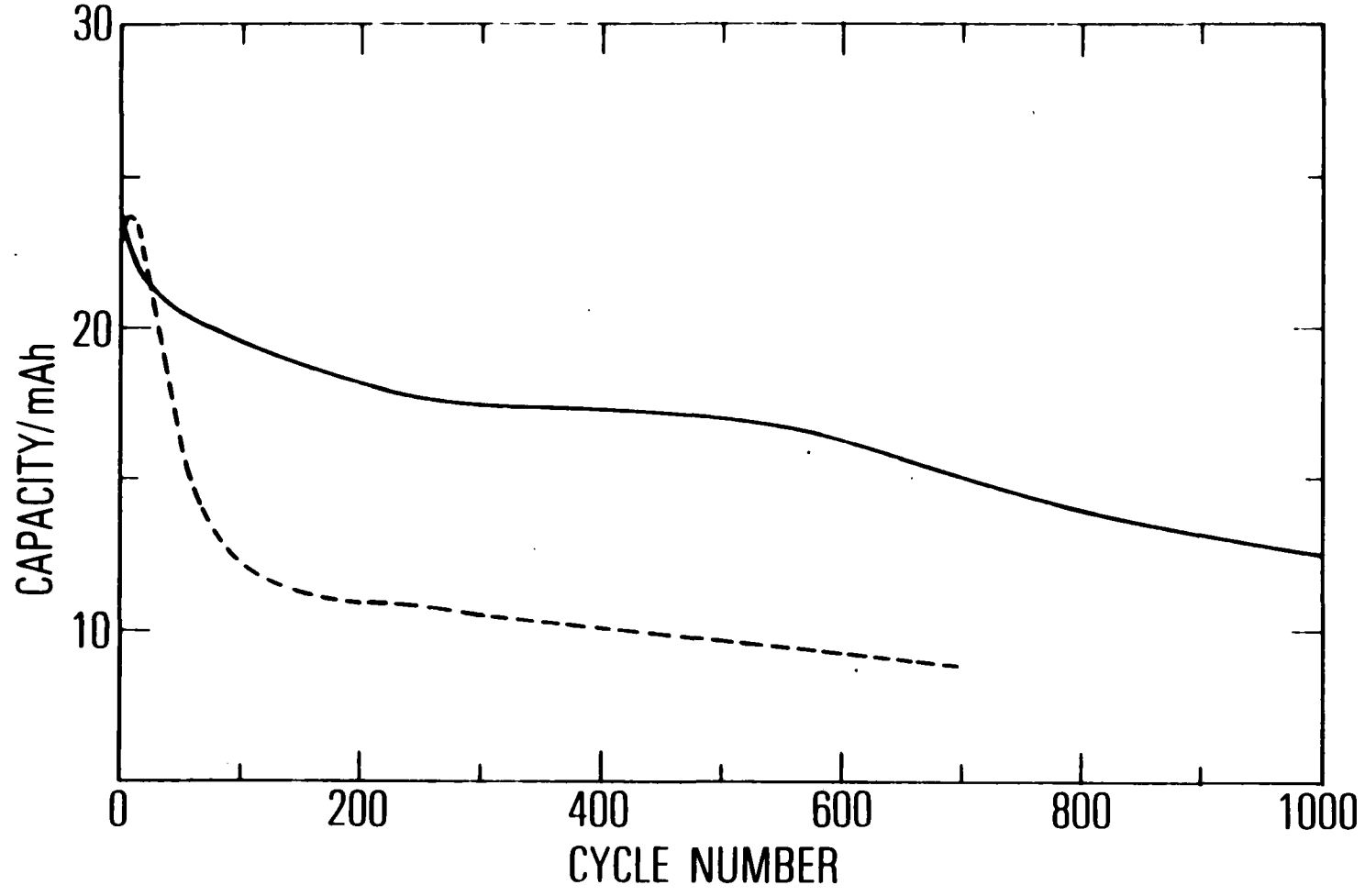

Fig. 11. Capacity as a Function of Cycle Number for Nickel Electrodes Containing 5% Mn (——) and 5% Zn (---). The initial theoretical capacities based on a one electron change are 28.2 and 28.6 mAh, respectively. Charge and discharge rates are 150 mA/cm^2.

IV. CONCLUSIONS

The impedance characteristics of the sintered nickel electrode have been studied during discharge for several additives that have been reported to influence electrode performance. The mechanisms of nickel electrode discharge were found to be generally unchanged by any of the additives. The resistance to proton diffusion during discharge in the active material was decreased by Li and Co additives and increased by Li and Co additives. The charge transfer resistance was also decreased by Li and Co additives with the effect of these two additives together being the sum of their individual effects. The data suggest that Co additives may decrease resistance by injecting proton carrier defects into the nickel oxyhydroxide lattice, whereas the largely interstitial defects provided by Li additives (Barnard et al., 1981) provide a decreased activation energy for charge transfer. The resistance of the poorly conducting material formed as the electrode discharge product, which acts as an isolating layer at the end of high rate discharge, was decreased significantly only by Mn and Co and slightly by Li. These effects are likely to reflect changes in the electronic resistance of the semiconductor material formed as a discharge product.

The additives that were found to clearly lower and, therefore, improve the impedance characteristics of the nickel electrode were Li and Co, a result that is consistent with widely documented performance data for nickel electrodes. Other additives were found to give impedances that were similar to or greater than electrodes containing no additives. The data for additives other than Co or Li suggest that these effects can be explained by how the various additives affect the morphology of the active material deposit in the porous structure of the sintered electrode. In all cases the changes in performance and impedance characteristics during cycling were found to correlate with the variables in electrode fabrication that should influence the deposit structure and morphology (such as temperature and deposition rate). These studies indicate that the performance of nickel electrodes is, in general, quite sensitive to several process parameters than can influence

the physical structure of the active material deposit in the porous electrode, and that the active material structure is dependent on additive type. Both Co and Li additives appear to make electrode performance less sensitive to variations in uniformity that can occur during fabrication, largely by virtue of the lower resistance that they create in the active material at a given state of charge.

REFERENCES

1. Barnard, R., Randall, C. F., and Tye, F. L., J. Applied Electrochem. 11, 517 (1981).

2. Beauchamp, R. L. and Maurer, D. W., "Extended Abstracts of the Fall Meeting of the Electrochemical Society, Battery Division" (1971), p. 23.

3. Casey, E. J., Dubois, A. R., Lake, P. E., and Moroz, W. Z., J. Electrochem. Soc. 112, 371 (1965).

4. Edison, T. A., U. S. Patent No. 876,445 (1907).

5. Fritts, D. H., J. Power Sources 6, 171 (1981).

6. Fritts, D. H., J. Electrochem. Soc. 129, 118 (1982a).

7. Fritts, D. H., The Nickel Electrode, R. G. Gunther and S. Gross, eds., The Electrochemical Society, Inc., Proceedings Vol. 82-4 (1982b), p. 175.

8. Jost, E. M., U. S. Patent No. 3,615,833 (1971).

9. Kelson, P., Sperrin, A. D., and Tye, F. L., Power Sources 4, 201 (1973).

10. MacArthur, D. M., J. Electrochem. Soc. 117, 422 (1970a).

11. MacArthur, D. M., J. Electrochem. Soc. 117, 929 (1970b).

12. Madou, M. J. and McKubre, M. C. H., J. Electrochem. Soc. 130, 1056 (1983).

13. Maladin, O. G., Vasev, A. V., Bityutskii, P. N., Shamina, I. S., and Suchkova, G. V., Electrokhim, 14, 91 (1978).

14. Pilla, A. A., J. Electrochem. Soc. 117, 729 (1970).

15. Ritterman, P., Lerner, S., and Seiger, H., Investigations of Battery Active Nickel Oxides, NASA CR-72128, NAS3-7620 (1966).

16. Takehara, Z., Kato, M., and Yoshizawa, S., Electrochim Acta. 16, 833 (1971).

17. Volynskii, V. A. and Chernykh, Y. N., Elektrochim. 13, 1874 (1970).

18. Weininger, J. L., General Electric Report S-70-1025, Dept. of Air Force Project No. 3145 (1970).

19. Weininger, J. L., The Nickel Electrode, R. G. Gunther and S. Gross, eds., The Electrochemical Society, Inc., Proceedings Vol. 82-4 (1982), pp. 6-8.

20. Zimmerman, A. H. and Janecki, M. C., The Nickel Electrode, R. G. Gunther and S. Gross, eds., The Electrochemical Society, Inc., Proceedings Vol. 82-4 (1982), p. 199.

21. Zimmerman, A. H. and Effa, P. K., J. Electrochem. Soc. 131, 709 (1984).

LABORATORY OPERATIONS

The Laboratory Operations of The Aerospace Corporation is conducting experimental and theoretical investigations necessary for the evaluation and application of scientific advances to new military space systems. Versatility and flexibility have been developed to a high degree by the laboratory personnel in dealing with the many problems encountered in the nation's rapidly developing space systems. Expertise in the latest scientific developments is vital to the accomplishment of tasks related to these problems. The laboratories that contribute to this research are:

Aerophysics Laboratory: Launch vehicle and reentry fluid mechanics, heat transfer and flight dynamics; chemical and electric propulsion, propellant chemistry, environmental hazards, trace detection; spacecraft structural mechanics, contamination, thermal and structural control; high temperature thermomechanics, gas kinetics and radiation; cw and pulsed laser development including chemical kinetics, spectroscopy, optical resonators, beam control, atmospheric propagation, laser effects and countermeasures.

Chemistry and Physics Laboratory: Atmospheric chemical reactions, atmospheric optics, light scattering, state-specific chemical reactions and radiation transport in rocket plumes, applied laser spectroscopy, laser chemistry, laser optoelectronics, solar cell physics, battery electrochemistry, space vacuum and radiation effects on materials, lubrication and surface phenomena, thermionic emission, photosensitive materials and detectors, atomic frequency standards, and environmental chemistry.

Computer Science Laboratory: Program verification, program translation, performance-sensitive system design, distributed architectures for spaceborne computers, fault-tolerant computer systems, artificial intelligence and microelectronics applications.

Electronics Research Laboratory: Microelectronics, GaAs low noise and power devices, semiconductor lasers, electromagnetic and optical propagation phenomena, quantum electronics, laser communications, lidar, and electro-optics; communication sciences, applied electronics, semiconductor crystal and device physics, radiometric imaging; millimeter wave, microwave technology, and RF systems research.

Materials Sciences Laboratory: Development of new materials: metal matrix composites, polymers, and new forms of carbon; nondestructive evaluation, component failure analysis and reliability; fracture mechanics and stress corrosion; analysis and evaluation of materials at cryogenic and elevated temperatures as well as in space and enemy-induced environments.

Space Sciences Laboratory: Magnetospheric, auroral and cosmic ray physics, wave-particle interactions, magnetospheric plasma waves; atmospheric and ionospheric physics, density and composition of the upper atmosphere, remote sensing using atmospheric radiation; solar physics, infrared astronomy, infrared signature analysis; effects of solar activity, magnetic storms and nuclear explosions on the earth's atmosphere, ionosphere and magnetosphere; effects of electromagnetic and particulate radiations on space systems; space instrumentation.

END

FILMED

1-86

DTIC